Title

Pathways for oxygen-isotope exchange in two model oxide clusters

Journal

New Journal of Chemistry, 40(2)

ISSN

1144-0546

Authors

Casey, William H

Rustad, James R

Publication Date

2016

DOI

10.1039/c5nj00985e

Peer reviewed

NJC

PERSPECTIVE

View Article Online
View Journal | View Issue

Cite this: *New J. Chem.*, 2016, **40**, 898

Pathways for oxygen-isotope exchange in two model oxide clusters

William H. Casey[ab] and James R. Rustad[c]

Studies of oxygen-isotope-exchanges in two classes of polyoxoions have uncovered some similarities in reaction steps that are also consistent with mineral-dissolution studies. The molecules were polyoxocations of Group 13 and polyoxoanions of Group 5, and the work was motivated by a desire to understand the dissolution of oxide minerals at the molecular scale. Experimentally, oxygen-isotope-exchange rates are found to be intensely sensitive to single-atom substitutions in the structures, even at sites that are otherwise inert. Exchange rates for different structural oxygen sites span several orders of magnitude, yet most oxygens within a molecule exhibit similar pH dependencies to isotopic exchange and these seem to reflect an average proton affinity of the ion. Single-atom substitutions have a dramatic affect on both the pH dependences of oxygen-isotope-exchanges and the overall reactivity of oxygen sites. Molecular dynamic and electronic-structure calculations identify similar steps in the pathways for exchange – (i) solvation forces cause a near-surface metal to detach from an underlying overbonded oxygen. (ii) This newly undercoordinated metal adds an isotopically normal oxygen as either a water, a hydronium ion or an hydroxide ion. (iii) Protons transfer from these adducts to more basic oxygens in the metastable structure. (iv) The metastability is longlived but access to the metastable state depends on the composition and symmetry of the starting structure, which is why single-atom substitutions are so important. (v) Within the metastable structure, oxygens shuffle positions and the metastable state collapses back into a more stable form. Pathways to form these metastable structures depend on the symmetry and composition of the starting geometry, which probably can't be adequately constrained for meaningful simulation at mineral surfaces.

Received (in Montpellier, France) 20th April 2015,
Accepted 22nd June 2015

DOI: 10.1039/c5nj00985e

www.rsc.org/njc

Introduction

There is enormous interest in understanding the dissolution of minerals and glasses in water at the molecular scale by geochemists and glass chemists concerned about the stability of things like waste forms for radioactive waste isolation, as well as to identify factors controlling the enhanced chemical durability of glass used in industry and life sciences. This interest has largely been manifested in bulk studies of solids in water followed by molecular-simulation of hydrolysis at the molecular scale. These studies are often attempts to identify single rate-controlling steps or activated complexes that can be used to inform the applied rate laws, which are usually based solely on the chemical affinities and an assumed form.

What has been missing from these studies are experiments and simulation at the same molecular scale, and yet polyoxometalate ions (POMs) have structures that are similar to condensed oxide phases and can be used as molecular models of the oxide–water interface. Here we review two careful studies that couple clusters with single-atom substitutions to reactive molecular-dynamic models. Both studies emphasize the importance of access to low-energy metastable states.

Broad features of oxide mineral dissolution

There have been enough studies of mineral oxide dissolution to identify some general features. First, for structures that do not have a polymerized oxide network, the dissolution rates scale like the familiar reactivity trends for other ligand-exchange reactions affecting the same octahedrally coordinated metals [Fig. 1]. The rates of dissolution of unpolymerized structures (*e.g.*, simple oxide (MO), orthosilicate (M_2SiO_4) or carbonate phases (MCO_3)) in identical solutions resemble the reactivity trends for other simple ligand-exchange reactions. A direct comparison is to rates of ligand-exchange of bound and bulk waters around the corresponding metal ions. The reason isn't

[a] *Departments of Chemistry, University of California Davis, One Shields Ave, Davis, CA 95616, USA. E-mail: whcasey@ucdavis.edu*
[b] *Department of Geology, University of California Davis, One Shields Ave, Davis, CA 95616, USA*
[c] *Corning Incorporated, One Science Center Drive, SP TD 01-1, Corning, NY 14831, USA. E-mail: rustadjr@corning.com*

mysterious – both metal detachment from a dissolving step and water exchange around an ion are oxide ligand exchanges affecting an octahedrally coordinated metal. Magnesium is octahedrally coordinated to oxygens in both the mineral forsterite [Mg_2SiO_4] and the ion released by acid-dissolution of forsterite, $[Mg(OH_2)_6]^{2+}$. Replacement of bridging oxygens with terminal oxygens is a sequence of similar ligand-exchange processes and the familiar reactivity trends abide. The rates of ligand exchange around d^8 Ni(II) are slower than around d^5 Mn(II) or d^{10} Zn(II) because of the crystal-field energies.[1–3] None of these minerals have extended and resistant oxide polymers. The orthosilicate minerals have isolated silicate tetrahedra, for example.

What is different for minerals is the averaging effect of composition. Also shown in Fig. 1(a) are the rates of dissolution at pH = 2 of mixed-metal orthosilicate minerals like monticellite [$CaMgSiO_4$]. Note that the Ca(II) is *not* rapidly leached out of the surface to leave a material that dissolves at the slow rate of forsterite [Mg_2SiO_4]. Instead the material dissolves at a rate given by the weighted expectations of composition. Composition in mixed-metal oxides exhibits a rate that is the weighted sum of the end member compositions. Of course such averaging effects of composition do not occur if the structure is modified by the substitution or of the metals don't substitute into homologous sites, as in clays.

Another interesting feature of oxide mineral dissolution kinetics is that the pH dependence of the rates is broadly amphoteric. In Fig. 1(b) we show the rates for dissolution of the mineral albite, $NaAlSi_3O_8$, which has been extensively studied.[4–7] This mineral has a silicate framework, although the amphoteric dissolution rate is observed for most oxides. Note that the rates increase in acidic solutions and in basic solutions and reach a minimum at near-neutral pH conditions. Molecular speculation about the causes of this pH dependence for minerals have given rise to dozens or hundreds of papers based largely on DFT simulations of purported activated states,[8–13] with little clarity shed.

In other words such dissolution rates exhibit a broadly amphoteric chemistry, as is typical for oxides in water. Rates are enhanced by adsorbed protons, or positive surface charge. Sometimes rates are also by adsorbed hydroxide ions or negative surface charge and there is a region where the rates vary poorly with solution pH. The molecular details are largely speculative. Of course, the observation is relevant to condensed oxide structures that do not exhibit a profound asymmetry in bonding, such as is found in clays, and that do not undergo selective leaching of some cations while the structure is intact. It is clear that the basic features of step-flow theory applies to minerals – reactions are *via* reaction at kink sites and the excavation of lattice defect outcrops, making etch pits. However these models are not molecular but arise from geometry and the juxtaposition of surface energies *via* the Gibbs–Thomson effect and bulk energies. They are basically geometric models for stacking cubes.

An additional interesting feature of mineral dissolution kinetics is the puzzling role of counterions. The rates seem to depend on the type and concentration of counterions beyond the effect that electrolyte concentration has on proton- and hydroxide-ion uptake.[14] One expects counterions to affect Brønsted acidities, but the effect seems to be about a factor of two larger.

What we can show in the next section is that these broad features of oxide mineral dissolution are also recaptured in the rates of oxygen-isotope exchanges and dissociations of simple polyoxoions that have a few dozen atoms. In these nanometer-sized ions, the pathways are *via* metastable equilibrium with a partly detached form of the molecule. Because charge-separation is implicit, counterions are important and the pathways involve the average proton affinities of the structure, not those of a single imagined bond that must be activated. Atoms in the structure react in concert.

William H. Casey

William Casey is a Distinguished Professor at UC Davis, with appointments both in the Department of Chemistry and the Department of Earth and Planetary Sciences. He takes immense pleasure in experimental work, particularly in collaboration with others.

James R. Rustad

Jim Rustad is a Research Associate in the Modeling and Simulation group at Corning Incorporated. He got his PhD in 1991 from the University of Minnesota (Geophysics) where he worked with David Yuen on silicate melts at high pressure and J. Woods Halley and Aneesur Rahman on one of the first reactive molecular dynamics models for water. In previous appointments at Pacific Northwest National Laboratory, the University of California, Davis and now also at Corning, he has been actively involved in development of reactive force fields for water–oxide systems, using this capability to investigate reaction mechanisms at mineral/glass–water interfaces.

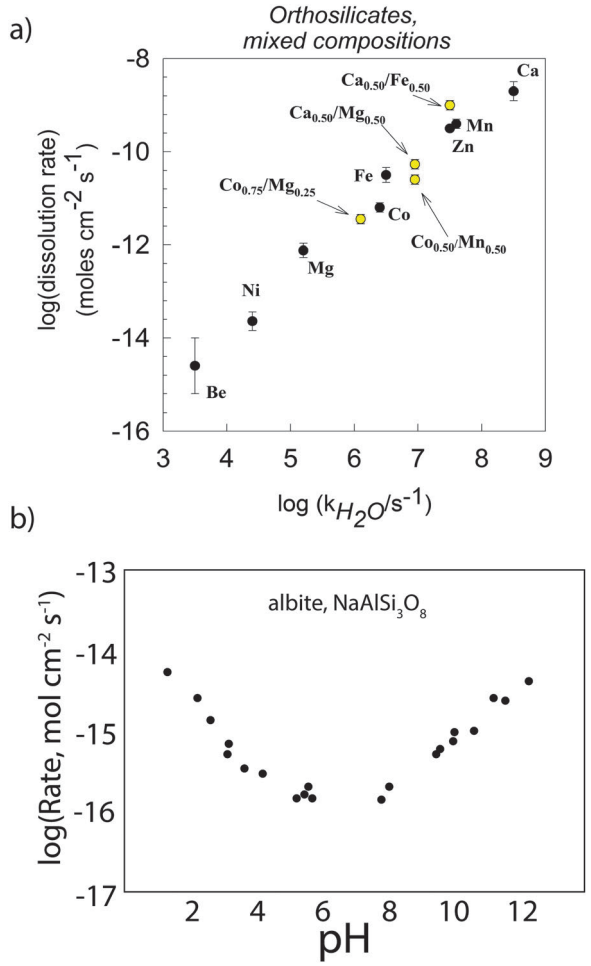

Fig. 1 (a) The dissolution rates at pH = 2 of a set of orthosilicate minerals,[1–3] with the stoichiometry: M_2SiO_4(s) and isolated SiO_4^{4-} tetrahedra. The abscissa is the rate of exchange of water from the corresponding metal ion (*e.g.*, Mg^{2+}(aq)) and the ordinate is the dissolution rate of the mineral (*e.g.*, Mg_2SiO_4, forsterite) normalized to area. The mixed-metal compositions are shown in yellow and are plotted against the weighted sum of the logarithms of rates of water exchange. (b) The dissolution rates are amphoteric for the aluminosilicate mineral albite ($NaAlSi_3O_8$), which has a tectoaluminosilicate framework structure.[4]

Oxygen-isotope-exchange pathways in nanometer-sized clusters

What is key in the model systems is that the dissociation of the ion can be detected unequivocally. In both of the examples systems, there is a set of oxygens that undergo isotopic substitution only when the molecule dissociates completely and reforms from the solvent. Thus, it is clear that isotope exchange at the other oxygen sites proceeds without dissociating the molecules.

$[MO_4Al_{12}(OH)_{24}(OH_2)_{12}]^{7/8+}$ ions of the ε-Keggin structure

The ε isomer of the Baker–Figgis–Keggin has one set of bound waters, two sets of 12 each of μ_2-OH and one set of μ_4-O in the center of the molecule. These μ_4-O bind the central tetrahedral metal (MO_4) to the outer part of the molecule and the octahedrally

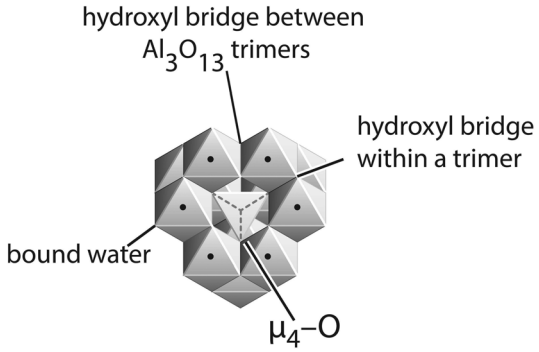

Fig. 2 The $[MO_4Al_{12}(OH)_{24}(OH_2)_{12}]^{7/8+}$ ion (MAl_{12}) has two sets of μ_2-OH that differ in their positions either between or within a Al_3O_{13} trimeric group. These groups rotate to make up the various isomers of the Keggin structure and this molecule has the ε-Keggin structure. Central to the molecule is a tetrahedrally coordinated metal, M = Al(III), Ga(III) or Ge(IV), that is bonded to μ_4-O that are inert to exchange. There are twelve bound waters that exchange with bulk solution in millisecond timescales.[15]

coordinated Al(III) metals ($Al(O)_6$). The ions have the stoichiometry: $[MO_4Al_{12}(OH)_{24}(OH_2)_{12}]^{7/8+}$ and M could be Al(III)(Al_{13}), Ga(III)($GaAl_{12}$)or Ge(IV)($GeAl_{12}$). The μ_2-OH fall into two groups, one set of twelve that are internal to the four trimeric entities and one set of twelve that link the trimeric entities to one another [Fig. 2].

Rates of oxygen-isotopic exchanges were determined *via* ^{17}O methods for the three molecules: Al_{13}, $GaAl_{12}$ and the Ge(IV)-substituted version: $GeAl_{12}$.[15–19] There are some key points that derive from these studies: (i) the μ_4-O and the central MO_4 sites are inert to substitution in the molecules.[20,21] These μ_4-O sites exchange oxygen isotopes with the bulk solution when the molecule dissociates completely and reforms. (ii) The bound waters exchange rates in the millisecond time scales and are nearly equal across the series; and (iii) the two sets of μ_2-OH differ by roughly a factor of $\sim 10^3$ in rates of isotopic exchange from one another within a single molecule. Without knowing anything specific about the mechanism, one could guess that the set of μ_2-OH within a trimeric group are probably the slowly reacting set and the μ_2-OH that link trimeric groups together are probably the rapidly reacting set, just based on general ideas about accessibility to water molecules. More complete understand of the mechanism provided by molecular modelling, as described below, strongly confirms that this is the case.

Most interestingly, (iv) the rates of oxygen-isotope exchange for similar oxygens across the series varies: $GeAl_{12} > Al_{13} > GaAl_{12}$ and the range is enormous. One set of μ_2-OH in the $GeAl_{12}$ is too reactive to even measure in an NMR experiment. The remaining μ_2-OH span a range of $\sim 10^7$ in rates of isotopic exchange, and are probably much larger if both sets of the $GeAl_{12}$ could be included. No pH dependence was detected although the range that could be covered was quite small. The key result was that a metal substituted into the inert core of these molecules has an enormous effect on the rates of isotopic exchange, even in parts of the molecule three bonds away.

This extraordinary sensitivity of the rates of steady oxygen-isotope exchanges was explained by examining the results of

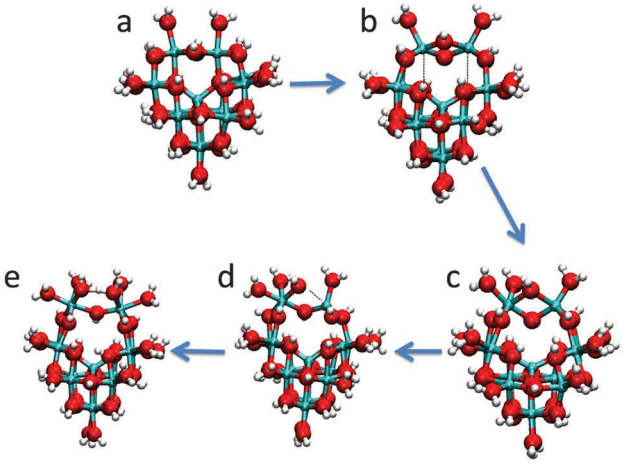

Fig. 3 Steps in conversion of Al_{13} to a metastable state.[22–24] Oxygen atoms are red, aluminum atoms are cyan, hydrogen atoms are white. Dashed lines represent key bond breaking events. (a) Stable Al_{13}; (b) bonds from top aluminum ions to the m_4-oxo break creating 5-fold coordinated aluminum; (c) five-fold aluminum ion on left takes on water; (d) Al–O–Al bridge breaks, creating tetrahedral aluminum ion on the right; (e) tetrahedral aluminum on the right takes on two water molecules from solution to create a metastable state with six-fold coordinated aluminum ions that are connected by μ-oxo and H_3O_2 bridges.

molecular dynamic simulations[22] coupled to electronic-structure calculations [Fig. 3]. What the authors found was that the central metal (Al(III), Ga(III) or Ge(IV)) controls access to a more loosely packed form of the structure that was essential to the isotope-exchange reaction. Although none of these central metals were exchangeable, the pathway for isotopic substitution was *via* a dimer-like moiety that was partly detached form of the stable ε-Keggin structure. This metastable intermediate had a finite lifetime and was not a transition state. Steps in forming the metastable intermediate were: (i) partial detachment of a $Al(O)_6$ from the underlying μ_4-O that was bonded to the central MO_4; (ii) addition of an isotopically normal water to the newly undercoordinated Al(III); (iii) proton transfer from a bound water to form a μ_2-O_2H_3 bridge between Al(III) in the dimer-like structure; (iv) exchange of oxygens positions in the H_3O_2 bridge; and (v) collapse back into the stable ε-Keggin structure.

The reason that the central metals are important is because the strengths of the M–μ_4-O–Al(III) bonds alternate. When the central M–(μ_4-O) bond is weak, as in the case where M = Ga(III), the (μ_4-O)–Al(III) is strong, access to the dimer-like metastable form is diminished, and the exchange rate is reduced. When the M–(μ_4-O) is strong, as in the case where M = Ge(IV), the adjacent (μ_4-O)–Al(III) is weak, access to the dimer-like metastable form is enhanced and the exchange rate is increased. Isotope exchange only takes place *via* the loosely packed metastable dimer-like structure. The essential reactivity trend revealed in the simulations is consistent with the results of electronic-structure calculations that show that energies to make the dimer-like structure vary systematically in the order $GeAl_{12} < Al_{13} < GaAl_{12}$.

It is important to note that the metastable intermediate and isotope-exchange pathways could be identified because the symmetry of the ε-Keggin structure is high (T_d). There are only a couple of accessible metastable states that could reasonably allow isotopic exchange. This limited "target" structure could therefore be "discovered" with molecular-dynamic simulations before it was known, even qualitatively, what kind of structure would come out of the simulations, or, for that matter, even that a metastable state was being sought. Furthermore, the molecule is a cation and there was no detected Brønsted acid–base influences on the reaction in the stable form of the molecule – all important proton-transfer processes took place only in the dimer-like intermediate structure, when the μ_2-O_2H_3 bridge formed that preceded isotopic exchange. The experiment was so well posed and so site-specific that discovery of the mechanism *via* molecular modelling was almost inevitably successful. In a sense, the systematic $[MO_4Al_{12}(OH)_{24}(OH_2)_{12}]^{7/8+}$ substitution series allowed most of the "molecular modeling" to be done in an experimental forum. While this is what modern experimental chemistry is all about, examples of where this has been done on anything resembling a complex geochemical systems are very rare or even non-existent.

Single-atom-substituted decaniobate ions

In the case of the aluminum polyoxocation discussed above, the isotope-exchange pathways could be detected only because experiments could be compared for sets of isostructural molecules with a single-atom substitutions in the center. These profoundly affected the rates. Here we examine isotope-exchange kinetics in a set of decametallate structures that vary systematically in charge *via* single-atom substitutions. These single-atom substitutions modify the reactivities of oxygens to isotopic substitution, but also dramatically affect the pH variations in rates.

It is best to introduce the experimental results stepwise, starting with the decaniobate ion: $[H_xNb_{10}O_{28}]^{(6-x)+}$. The niobates were chosen for study only because the metal does not undergo changes in redox state in water and because the rates of oxygen-isotope exchanges were slow enough to be conveniently followed using ^{17}O NMR methods.[25–32]

To follow steady rates of oxygen-isotope exchange in this molecule, Villa *et al.* prepared versions from 40% ^{17}O-enriched water so that all oxygens in the molecule were tagged and then precipitated it as a salt with tetramethyl ammonium cation. This salt was then dissolved into isotopically normal water and the seven signals were identified and followed as a function of time. These seven signals corresponded to the seven oxygen sites in the decaniobate structure and varied in field position according to bonding. The most upfield peak was assigned to the two central μ_6-O (Site A) in the molecule and the most downfield peaks were the two sets of η = O, labeled G and F in Fig. 4(a). In between were three sets of μ_2-O (C, D, and E) and one set of μ_3-O (Site B). Diminution of the ^{17}O NMR peaks for these sites yields the rates of isotopic substitution and the constant signal for Site A, the central μ_6-O, indicates that the molecule is stable.

What is found for this ion is that the oxygen sites exchange at rates that differ by 10^3–10^4 from one another, but that they all exhibit the same pH dependence. Rates increase dramatically

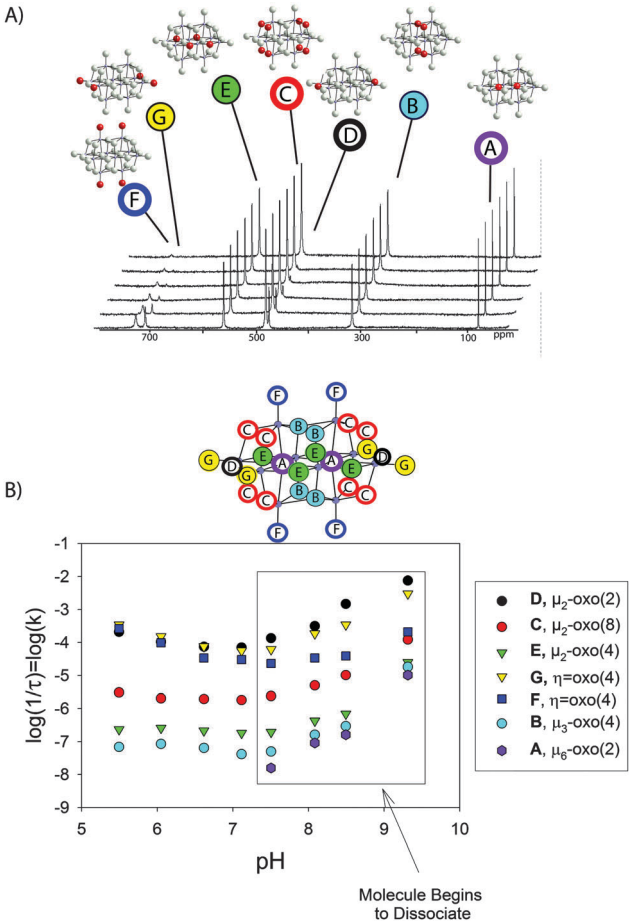

Fig. 4 (A) The decaniobate ion, $[H_xNb_{10}O_{28}]^{(6-x)+}$, has seven oxygen sites and three metal sites.[28,30,33] The oxygen type and number are color coded and the atoms are identified with red in (B) oxygens are in two central μ_6-O (Site A), four μ_3-O (Site B), three sets of μ_2-O (C, D, and E) and two sets of η = O, labeled G and F. The ^{17}O peaks for these sites (A) are easily resolved in an NMR spectrum and changes in intensity with time, shown above in a stacked plot, yield the rates of isotopic exchange with the solution (B). At pH > 7.5, diminution of the signal from the ^{17}O in Site A, the central μ_6-O, indicates that the molecule is dissociating.

with $[OH^-]$ concentration at pH > 7, but in tandem. The pH dependence is also in tandem with the very slow rate of dissociation of the molecule, which is detectable at pH > 8.5.

From titrations, Villa *et al.*[26,30,33] estimated that the molecule is unprotonated beyond pH ~ 6. From mass-spectroscopy and NMR data, it is found that the molecule dissociates by cleavage into a hexamer and tetrameric fragments *via* rupture at the μ_3-O site.[33,34] The pathway was discovered because transfer of the ^{17}O tag from the mother to the daughter ions can be identified in NMR spectra. This dissociation of the decametallate into hexamer and tetrameric fragments is probably reversible, because the ^{17}O tag diminishes with time after dissociation as though the decaniobate were reforming and cleaving repeatedly with a 50% chance of transferring the ^{17}O at each dissociation.

The key observations are: (i) whatever causes the $[H_xNb_{10}O_{28}]^{(6-x)+}$ molecule to dissociate, measured by the loss of signal from the central μ_6-O, Site A, also causes the exchange of oxygen isotopes into the six reactive oxygens (Sites B–G); and (ii) the entire structure is involved in isotope-exchange pathways. This behaviour differs strongly from what might have been expected based on a "functional-group" perspective. From such a perspective it would have been guessed that there are sites of high proton affinity that would be activated through protonation and that these would be completely different sites than those activated by OH^- nucleophilic attack. In this view the sites of reaction are isolated from one another. In contrast, the experimental work indicates that there are no isolated functional groups, save possibly for the bound waters, which are relatively insensitive to small changes in composition and structure.

The charge of the molecule can be changed by substituting Ti(IV) for Nb(V) in the central part of the molecule, making an isostructural form of the decaniobate, but with the stoichiometry: $[H_xNb_8Ti_2O_{28}]^{(8-x)+}$. The oxygen-isotope-exchange rates for the seven oxygens were followed *via* NMR and one could see that the pH dependencies were again the same for all oxygens in the molecule, but now the pH dependence for the rates is inverted [Fig. 5]. All oxygens now have rates that increase with proton concentration, yet still differ by the factor of by 10^3–10^4 from one another. The pH dependence was completely inverted by the simple substitution of two Ti(IV) for Nb(V) in the center.

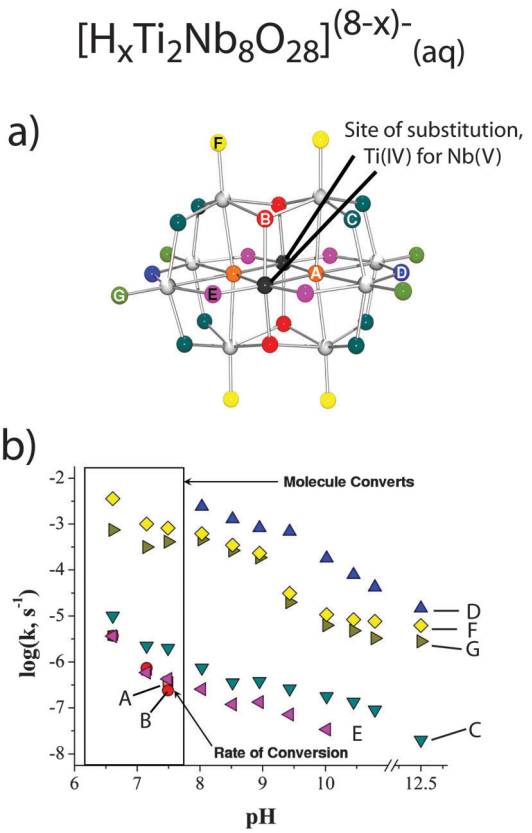

Fig. 5 (a) When the charge of the decaniobate ion is increased by Ti(IV) ⇒ Nb(V) substitution, the pH dependencies for the rates of oxygen-isotope-exchanges invert (b) relative to the decaniobate ion ($[H_xNb_{10}O_{28}]^{(6-x)+}$). As with the decaniobate ion, all oxygens exhibit the same pH dependence, although now the reaction is proton-enhanced instead of being enhanced by hydroxide ion and increased pH.[30]

Then, to make the series complete, Villa *et al.* also synthesized a version of the molecule with a single atom substitution, again Ti(IV) for one Nb(V), in the center of the structure and with no nonbridging oxygens, making the $[H_xNb_9TiO_{28}]^{(7-x)+}$ ion. Again rates for all oxygen sites exhibited the same pH dependence and the total range was 10^3–10^4. However, now the rates of exchange were clearly broadly amphoteric – rates increased with $[OH^-]$ concentration at pH > 10.5 and with $[H_3O^+]$ at pH < 10. Thus the complete inversion of pH dependence seen for the dititano complex was simply a result of shifting the "pH of minimum oxygen exchange rate" to higher pH. Although there is no real reason to expect it, even the approximately $\sim 10^2$ increase in rate at the extreme ends of the amphoteric curve agrees almost exactly with what is seen for albite in Fig. 1b. The rates of a single oxygen near or far from the site of substitution were surprisingly similar – the C Site (a μ_2-O at the corner of the molecule) had rates within about a factor of 2–3 depending on the proximity to the site of Ti(IV) substitution.

These experiments on a nanometer-sized molecule have important things to tell geochemists interested in understanding oxide reactions at the molecular scale. What these experiments show is that the overall charge of the molecule, its overall proton affinity, controls the pH dependence for oxygen-isotope-exchange rates. All oxygen sites exhibited a similar pH variation within a single composition molecule ($[H_xNb_{10}O_{28}]^{(6-x)+}$, $[H_xNb_9TiO_{28}]^{(7-x)+}$ or $[H_xNb_8Ti_2O_{28}]^{(8-x)+}$ ions). This pH variation is identical to the pH dependence of the dissociation rate of the molecule. The local effects of composition were muted and, although we do not show it here, counterions have a regiospecific effect on rates of oxygen-isotope exchanges. The presence of borate ion, for example, enhances the rates of exchange of the C Site, a μ_2-O on the corner of the molecule by about 10^2 but has no effect on the E Site, a μ_2-O in the equatorial plane of the molecule. This regiospecificity is very interesting because the rates of oxygen-isotope exchanges in borate ion, or boric acid, are much, much faster than the rates of exchange of the oxygens. The effect of these counterions must be electrostatic in nature; they are much too reactive to be linking to the reactive oxygens at the niobate ion.

Oxygen-stuffing reactions involving all atoms

These two sets of model ions discussed above, either the aluminum-hydroxide cations or the niobate anions, are the same size, or actually larger than, the clusters that are used in *ab initio* simulations to understand the dissolution rates of minerals and glasses.[12] What the experiments show is that these entire molecules respond to changes in solution composition and all atoms are involved in the isotope-exchange pathways. The niobate experiments show that isotope-exchange rates are broadly amphoteric [Fig. 6], as is found in the dissolution rates of many oxide and aluminosilicate minerals and solids. The decaniobate ion is a weak base and only picks up a proton at pH < 7, yet this protonation causes *sets* of structural oxygens to react quickly. In other words, and in contrast to long-held opinions about proton-enhanced bond ruptures, the effect of protonation of the molecule is not limited to the surface oxygen reacting with an incoming water. As dissociation of the molecule increases with pH, the isotope-exchange rates for *all* structural oxygens increase in parallel, even if they react many orders of magnitude more rapidly than dissociation.

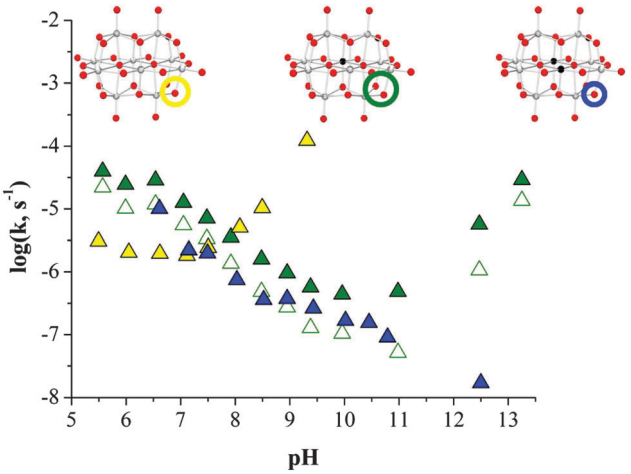

Fig. 6 The rates of oxygen-isotope-exchange in Site C (a μ_2-O at the corner of the molecule) for the decaniobate ion ($[H_xNb_{10}O_{28}]^{(6-x)+}$), a version with a single atom substitution of Ti(IV) for Nb(V) making the $[H_xNb_9TiO_{28}]^{(7-x)+}$ and a version with two Ti(IV) for Nb(V) substitutions, again in the central metal site, making the $[H_xNb_8Ti_2O_{28}]^{(8-x)+}$ ion.[28] Note that whether the reaction is proton-enhanced, hydroxide-enhance or unenhanced depends only on the charge of the molecule (+6, +7 or +8) in its unprotonated form. Although we show only the C Site, all oxygens in these molecules exhibit the same pH dependence to their rates of isotopic exchange with the bulk solution, and these rates are much faster than the rates of dissociation of the molecule (see Fig. 4).

Simulations of the reactions were conducted using both molecular-dynamic methods and electronic-structure calculations. These simulations uncovered a set of steps that seem to be common. For the niobate ions, as with the aluminum-hydroxide cations, there were sets of low-energy metastable structures that formed and that had a finite lifetime – they were not transition states but rather metastable forms of the molecule that allowed isotopic exchange and, in the case of high energies, dissociation into products [Fig. 7].

In the niobate molecules, these metastable structures formed by facile nucleophile additions that are enabled by retraction of metals from underlying highly coordinated oxygen atoms. The reactions begin by partial detachment of a surface atom like Nb(V) from the highly coordinated μ_6-O (Site A). This detachment was mitigated by solvation forces but could be influenced by protonation state of the cluster. As the metal detaches, a nucleophile enters the inner-coordination-sphere of the newly detached Nb(V) metal and these nucleophiles could be either a water molecule, a hydronium ion or a hydroxide ion. Protons from the nucleophile could be transferred to, or from, other more basic oxygens in the metastable structure. In this way, structures of the intermediates formed by adding water, OH^- and H_3O^+ tended to ultimately come to resemble one another – the protons were transferred to other oxygens in the metastable state. In other words, the proton-enhanced rates increase because the proton facilitates the hydration, or addition of a water molecule to the structure, promoting the formation of the

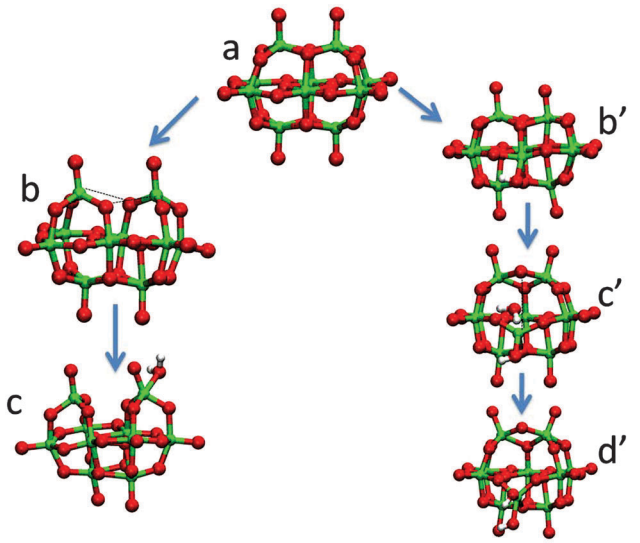

Fig. 7 Two different pathways for conversion of decaniobate ion to a metastable state. Oxygen atoms are red, Nb(v) atoms are green, hydrogen atoms are white. Dashed lines represent key bond-breaking events. (a) Stable structure. Left path: (b) bonds from niobium ions to the μ_3-oxo break creating two four-fold-coordinated Nb(v) on the top of the molecular ion; (c) four-fold Nb(v) ion on right takes on water; Right path: (b′) nucleophilic attack of hydroxide ion from below begins to pull the central metal out from its "lattice" position; (c′) an additional water molecule pulls the central Nb(v) atom completely out of its lattice position, severing the bond to the top μ_3-oxo. (d′) Added water in (c′) deprotonates making metastable state with five-fold coordinated Nb(v) in the center.

same metastable state that would be produced from hydroxide addition. In this way, proton-promoted enhancement of oxygen exchange rates can be regarded as hydronium ion addition even though the added unit may be added as separate $H_2O + H^+$ pieces.

For the decametallate structures, which have much lower symmetry than the MAl_{12} ions (T_d *versus* D_{2d} for the decaniobate ion), many more metastable structures could be found *via* these low-energy partial detachments. The adding of an oxygen to the metals was termed an 'oxygen-stuffing reaction' because the different nucleophiles yielded similar ultimate products.[35] Counterions are important, of course, because the formation of these metastable open structures involves transient charge separations which can be partially compensated by counterions as well as solvent. The proton affinities of oxygens in these metastable structures were not too different from one another and thus proton additions tend to labilize the entire molecule, not just a single bond, as the protons were shuffled among the more-basic oxygens.

Just as in the case for the $[MO_4Al_{12}(OH)_{24}(OH_2)_{12}]^{7/8+}$ ions, it was access to the metastable states that controls the rates of oxygen-isotope exchange and dissociation [Fig. 3 and 7]. All atoms are involved. Thus a view of the reaction that emphasizes only local hydrolysis and exchange is incorrect – at the nanometer size scale, all atoms are involved in an isotope-exchange reaction because they are all involved informing the relevant metastable state. The overall charge of the stable molecule reflects the affinity for protons and controls the pH of minimum oxygen exchange rate and pH dependence of the isotope-exchange reactions.

What this means for the mineral–fluid interface is that simulations that hope to capture the essential interface chemistry by using small cluster fragments are doomed to failure. Work on the nanometer-sized clusters indicates that the structure must be known and reproduced in the simulation to capture any of the essential pathways for reaction. All atoms are involved in the reaction and exert enormous influence on the outcome and energetics. Furthermore the number and the energetic details of the metastable states are quite sensitive to the symmetry of the starting geometry, which is well known for these nanometer-sized clusters but impossible to know at the step sites on reacting minerals.

These results have both good and bad news for scientists hoping to understand the molecular details of metal hydrolysis at mineral surfaces. The experiments described here show that these molecular pathway details are probably not knowable or important to understanding the dissolution reaction. A 40-atom cluster recaptures most of the reactivity trends observed for dissolving oxides (amphoteric chemistry, predictable dependence on composition) so that the actual structure of the metastable states forming on a step are now conceptually unimportant.

Conclusions and perspectives

These clusters capture the general features of dense oxide minerals dissolving in water *via* non-reductive pathways, amphoteric rates, strong influence of composition and minor influence of counterions. The pathways for isotope exchange and dissociation emphasize the importance of metastability, not activated bond ruptures. The formation of a metastable state in both cases involve similar steps: (i) a near-surface metal detaches from an underlying overbonded oxygen, such as the μ_4-O in the case of the $[MAl_{12}(OH)_{24}(OH_2)_{12}]^{7/8+}$ ions or the μ_6-O in the case of the $[H_xNb_{10}O_{28}]^{(6-x)+}$, $[H_xNb_9TiO_{28}]^{(7-x)+}$ or $[H_xNb_8Ti_2O_{28}]^{(8-x)+}$ ions. (ii) Counterions are important because the formation of the loose metastable state involves charge separation. The effects are regiospecific. (iii) Isotopically normal oxygen adds to the newly undercoordinated metal as either H_2O, OH^- or H_3O^+. (iv) Protons move to more basic oxygens in the intermediate structure, which has a long lifetime relative to the exchange event. (v) The isotopically normal oxygen shuffles within the metastable intermediate. For the Al_{13} ion this shuffling is *via* an μ_2-$O_2H_3^+$ bridge. (vi) The loose metastable form collapses back into the stable form of the molecule.

Single-atom substitutions are important because these control the access of the metastable state that is essential for isotopic exchange. Pathways to form these metastable structures depends on the symmetry and composition of the starting geometry. It is probably not possible to constrain sites for meaningful simulation at mineral surfaces because details of the starting structure must be known to great detail. For the oxygens we discuss here in these molecules, only the bound waters can be considered to react in isolation from other changes affecting the cluster structure.

Finally, the reactions steps in these examples could be detailed only because the experimental work was conducted

in tandem with simulation, and at the same site-specific scale. Both components of the study were essential as it would have been nearly impossible to infer the key pathways from intuition alone. Future work could focus on similar tandem studies of nanometer-sized oxides to great benefit. It would be interesting, for example, to see how the highly collective perturbations to the structure resulting in the metastable states postulated here would apply to more loosely packed precursor clusters, such as those seen in silicate and aluminosilicate oligomers. These systems may have much greater flexibility in accommodating oxygen-exchange pathways and might act in a more site-specific manner than the more closely packed polyoxometallate systems.

Acknowledgements

The authors are grateful to three careful referees and the editor for improvements to the work, which is supported by the Department of Energy grant DE-FG02-05ER15693.

Notes and references

1 H. R. Westrich, R. T. Cygan, W. H. Casey, C. Zemitis and G. W. Arnold, *Am. J. Sci.*, 1993, **293**, 869–893.
2 W. H. Casey and H. R. Westrich, *Nature*, 1992, **355**, 157–159.
3 W. H. Casey, *J. Colloid Interface Sci.*, 1991, **146**, 586–589.
4 L. Chou and R. Wollast, *Am. J. Sci.*, 1985, **285**, 963–993.
5 A. E. Blum and A. C. Lasaga, *Geochim. Cosmochim. Acta*, 1991, **55**, 2193–2201.
6 A. C. Lasaga and A. Lüttge, *Am. Mineral.*, 2004, **89**, 527–540.
7 A. Blum and A. Lasaga, *Nature*, 1988, **331**, 431–433.
8 Y. Xiao and A. C. Lasaga, *Geochim. Cosmochim. Acta*, 1996, **60**, 2283–2295.
9 Y. Xiao and A. C. Lasaga, *Geochim. Cosmochim. Acta*, 1994, **58**, 5379–5400.
10 J. D. Kubicki, Y. Xiao and A. C. Lasaga, *Geochim. Cosmochim. Acta*, 1993, **57**, 3847–3853.
11 C. P. Morrow, S. Nangia and B. J. Garrison, *J. Phys. Chem.*, 2009, **113**, 1343–1352.
12 S. Nangia and B. J. Garrison, *J. Phys. Chem.*, 2008, **112**, 2027–2033.
13 A. F. Wallace, G. V. Gibbs and P. M. Dove, *J. Phys. Chem. A*, 2010, **114**, 2534–2542.
14 M. Karlsson, C. Craven, P. M. Dove and W. H. Casey, *Aquat. Geochem.*, 2001, **7**, 13–32.
15 W. H. Casey, *Chem. Rev.*, 2006, **106**, 1–16.
16 W. H. Casey, B. L. Phillips, M. Karlsson, S. Nordin, J. P. Nordin, D. J. Sullivan and S. Neugebauer-Crawford, *Geochim. Cosmochim. Acta*, 2000, **64**, 2951–2964.
17 B. L. Phillips, W. H. Casey and M. Karlsson, *Nature*, 2000, **404**, 379–382.
18 W. H. Casey and B. L. Phillips, *Geochim. Cosmochim. Acta*, 2001, **65**, 705–714.
19 A. P. Lee, B. L. Phillips and W. H. Casey, *Geochim. Cosmochim. Acta*, 2002, **66**, 577–587.
20 T. H. Walter and E. Oldfield, *J. Phys. Chem.*, 1989, **93**, 6744–6751.
21 A. R. Thompson, A. C. Kunwar, H. S. Gutowsky and E. Oldfield, *J. Chem. Soc., Dalton Trans.*, 1987, 2317–2322.
22 J. R. Rustad, J. S. Loring and W. H. Casey, *Geochim. Cosmochim. Acta*, 2004, **68**, 3011–3017.
23 J. R. Rustad, in *Advances in Inorganic Chemistry*, ed. R. Van Eldik, Academic Press, 2010, vol. 62, pp. 391–436.
24 W. H. Casey and J. R. Rustad, *Annu. Rev. Earth Planet. Sci.*, 2007, **35**, 21–46.
25 E. M. Villa, C. A. Ohlin, J. R. Rustad and W. H. Casey, *J. Am. Chem. Soc.*, 2010, **132**, 5264–5274.
26 E. M. Villa, C. A. Ohlin and W. H. Casey, *Am. J. Sci.*, 2010, **310**, 629–644.
27 E. M. Villa, C. A. Ohlin and W. H. Casey, *Chem. – Eur. J.*, 2010, **16**, 8631–8634.
28 E. M. Villa, C. A. Ohlin and W. H. Casey, *J. Am. Chem. Soc.*, 2010, **132**, 5264–5272.
29 C. A. Ohlin, E. M. Villa, J. R. Rustad and W. H. Casey, *Nat. Mater.*, 2010, **9**, 11–19.
30 E. M. Villa, C. A. Ohlin, J. R. Rustad and W. H. Casey, *J. Am. Chem. Soc.*, 2009, **131**, 16488–16492.
31 E. M. Villa, C. A. Ohlin, E. Balogh, T. A. Anderson, M. Nyman and W. H. Casey, *Am. J. Sci.*, 2008, **308**, 942–953.
32 W. G. Klemperer and K. A. Marek, *Eur. J. Inorg. Chem.*, 2013, 1762–1771.
33 E. M. Villa, C. A. Ohlin, E. Balogh, T. M. Anderson, M. D. Nyman and W. H. Casey, *Angew. Chem., Int. Ed.*, 2008, **47**, 4844–4846.
34 P. Comba and L. Helm, *Helv. Chim. Acta*, 1988, **71**, 1406–1420.
35 J. R. Rustad and W. H. Casey, *Nat. Mater.*, 2012, **11**, 223–226.